Internal Dynamics of a Differentiated Ganymede: Constraints from experimental data. C. Sotin and S.L. Murchie, Dept. Geological Sciences, Brown University, Providence, RI, 02912.

Experiments on the creep behavior of high pressure ices (1,2,3) and characteristics of the phase transitions between the different water ice polymorphs (4), provide strong constraints to model the internal dynamics of a Ganymede-like icy satellite. At least three different phases of ice are likely to exist from the surface (ice I) down to the boundary with the silicate core (ice VI). Since the icy mantle is layered, and assuming that convection exists, an important question is whether subsolidus convection in this satellite is also layered. This study first shows that the transition ice II — ice VI (or ice V) is a major discontinuity which leads to layered convection. Then, parameterized convection for a layered mantle is developed. Embodying the experimental creep law, this model predicts the thermal structure of this satellite and its evolution with time.

Previous linearized stability analysis of this problem for icy satellites (5) has shown that the two most critical parameters are the viscosity of the different polymorphs of ice and the thickness of the layer, in which the phase transition is supposed to occur at the mid plane. Recently, we have developed a linearized stability analysis (6) which takes into account density and possible viscosity differences between the two phases, and which allows the two layers to have different thickness. Furthermore, this study showed that the viscosity of ice is not required to investigate this problem. The stability of a phase transition depends on two parameters R' and S which can be expressed versus the buoyancy parameter P, the ratio (X) between the linear thermal gradient and the adiabatic gradient, and the ratio (XI) between the slope of the Clapeyron curve and the adiabatic gradient: $R'=P/(X-1)$, $S=XI.P/(XI-X)$. The values of the buoyancy parameter are known from the experimental studies carried out to determine the phase diagram of ice (4).

Figure 1 displays the results for the transitions ice I — ice II, ice II — ice VI and ice II — ice V. Since the temperature difference between the top and the bottom of the layer is not known, we have investigated values of these parameters for different values of this difference. For a given linear thermal gradient (given value of X), we are able to deduce the depth of each phase transition and therefore the thickness of each phase. This provides the value of the buoyancy parameter and thus the value of R' and S which characterize the phase transition. Each phase transition can therefore be plotted in the phase transition plane (Figure 1). The heavy curve represents the phase transitions whose minimum critical Rayleigh number is equal to the value it would have if there were no phase transition. If the phase transition is in the dotted area, then it requires a smaller Rayleigh number. The phase transition therefore enhances convection. Otherwise, it requires an higher minimum critical Rayleigh number, which means that the phase transition is a barrier to convection. All the phase transitions, except those of ice I into ice II at high values of X, require higher Rayleigh numbers.

According to the position of the phase transition, the minimum critical Rayleigh number and the pattern of convection can be deduced. Figure 2 shows the convection pattern for the transition ice II into ice VI. Layered convection is predicted. A value of the minimum critical Rayleigh number can be inferred from the position of the phase transition in Figure 1, which yields a value of the viscosity for convection to occur. This value is reported in $(\log(X-1),\log(\mu))$ plot (curve 2 in Figure 3). In the same plot, the experimental creep law can be drafted (curve 1). The intersection between these two curves provides the linear thermal gradient and the related viscosity for convection to occur. Figure 3 suggests that convection begins for a very small value of the linear thermal gradient (less than two times the adiabatic thermal gradient).

In order to get the values of both the temperature difference and the viscosity at a steady-state, parameterized convection is applied to a layered mantle, using the same equation as for single cell convection (7). The viscosity difference between the two layers is determined according to the experimental activation energy (1). The evolution of the Nusselt number versus the minimum critical Rayleigh number and the Rayleigh number can be plotted in $(\log(X-1), \log(\mu))$ plot (Figure 3). The two curves (3) and (4) in this figure represent two values of heat production, one just after accretion, and the other at the present time. Experimental values of the viscosity can also be reported assuming a given value of the shear stress to account for the non-Newtonian rheology of ice. The intersection between the experimental curve and the Nusselt-Rayleigh curve provides both the viscosity and the temperature difference at a steady-state convection. The temperature profile can then be plotted and compared with the solidus curve (Figure 4).

In contrast to single cell models, this model predicts a very warm ice VI layer. The temperature at the ice II — ice VI transition is quite close to the melting temperature and suggests that partial melting may have occured in the past, when the heat flux was high.

 INTERNAL DYNAMICS OF A DIFFERENTIATED GANYMEDE

Sotin C. and Murchie S. L.

References: (1) Sotin, C. et al., in *Ices in the solar system*, ed. by J. Klinger, 1985. (2) Sotin, C. and J-P. Poirier, *Journal de Physique*, C1, 48, 233–238, 1987. (3) Durham, W.B. et al, *Journal de Physique*, C1, 48, 221–226, 1987. (4) Hobbs, *Ice physics*, Clarendon Press Oxford, 1974. (5) Bercovici, O. et al, *Geophys. Res. Let.*, 13, 448–451, 1986. (6) Sotin, C. and E.M. Parmentier, *Phys. Earth Planet. Int.*, submitted, 1988. (7) Stevenson, D.J. et al, *Icarus*, 54, 466–489, 1983.

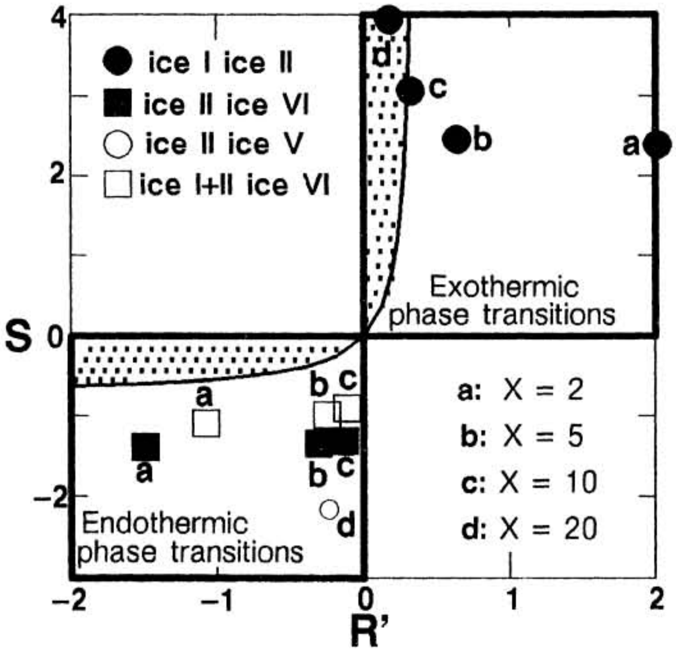

Figure 1: Position of the phase transitions into the phase transition plane. The heavy curve delimits phase transitions which enhance convection (dotted area) from phase transitions which act as barrier to convection.

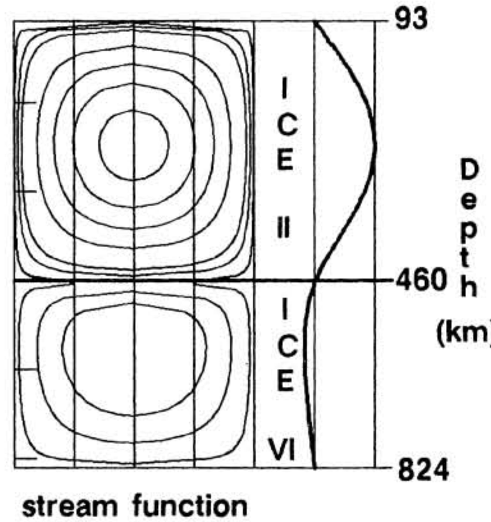

Figure 2: Convection pattern at the onset of convection for the transition ice II – ice VI Ra=6310, X=5. The vertical velocity profile is shown on the right.

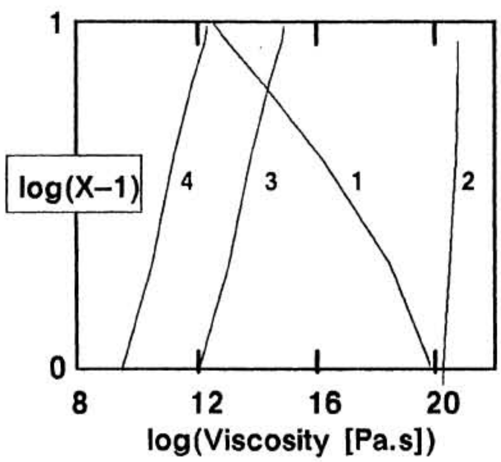

Figure 3: Temperature difference versus Viscosity
1: Experimental creep law. 2: Relation at the onset of convection. 3: Relation at a present time heat flow
4: Relation at post-accretional heat flow

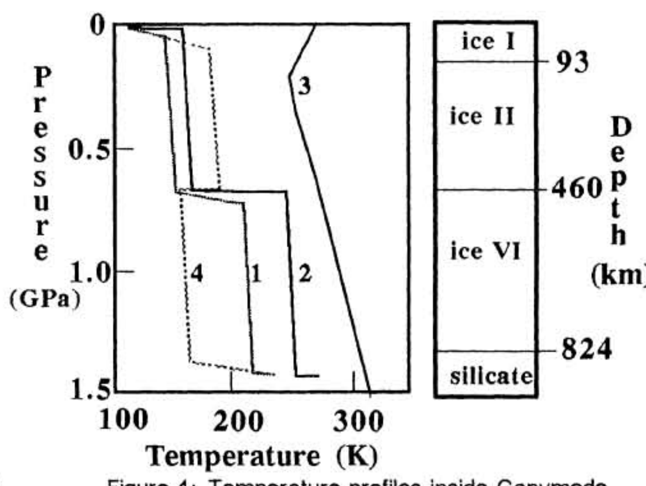

Figure 4: Temperature profiles inside Ganymede just after accretion (1), and at present time (2). (3) is the solidus curve. (4) is the temperature profile for single cell convection